



Anopheles gambiae Control and Antibacterial Activity of Silver, Gold, and their Alloy Nanoparticles Synthesized Using *Pleurotus ostreatus*

Elijah A. Adebayo^{1,2}, Muinat M. Ayantola^{1,2}, Hassan A. Balogun¹, Agbaje Lateef¹, Musibau A. Azeez¹, Taofeek A. Yekeen¹, Lorika S. Beukes³, Ntombozuko Matyumza⁴, and Evariste B. Gueguim-Kana³

¹Pure and Applied Biology Department, Ladoke Akintola University of Technology, P.M.B 4000, 210101, Ogbomoso, Nigeria

²Nanobiotechnology and Microbiology Laboratory, Room 35, New Biology Laboratory Complex, Ladoke Akintola University of Technology, 210101, Ogbomoso, Nigeria.

³Department of Microbiology, School of Life Sciences, University of KwaZulu-Natal, Private Bag X01, Scottsville, Pietermaritzburg 3209, South Africa

⁴Microscopy and Microanalysis Unit, School of Life Sciences, University of KwaZulu-Natal, Pietermaritzburg, South Africa

ARTICLE INFO

Article history:

Received 09 June 2025

Revised 25 August 2025

Accepted 01 September 2025

Published online 01 December 2025

Copyright: © 2025 Adebayo et al. This is an open-access article distributed under the terms of the [Creative Commons Attribution License](https://creativecommons.org/licenses/by/4.0/), which permits unrestricted use, distribution, and reproduction in any medium, provided the original author and source are credited.

ABSTRACT

Mosquitoes, the primary malaria vectors in Nigeria, have developed increasing resistance to synthetic insecticides, necessitating the search for eco-friendly alternatives. This study investigates the insecticidal and biomedical properties of silver nanoparticles (AgNPs), gold nanoparticles (AuNPs), and silver-gold alloy nanoparticles (Ag-AuNPs) synthesized via a green method using *Pleurotus ostreatus* extracts. Nanoparticles were characterized using UV-visible spectroscopy and Fourier-transform infrared spectroscopy (FTIR). Their larvicidal and pupicidal efficacy was tested at 1–30 µg/mL concentrations over 12 and 24 hours, while adult mosquitoes were exposed to nanoparticle-infused coil fumes. Additionally, antibacterial activity against eight clinical bacterial isolates was evaluated. UV-visible spectroscopy showed maximum absorbance at 430, 550, and 540 nm for AgNPs, AuNPs, and Ag-AuNPs, respectively, while FTIR analysis confirmed functional group interactions at 3778, 3262, and 3037 cm⁻¹. Mortality increased with concentration and exposure time, with a maximum effect at 170 µg/mL for adult mosquitoes. Antibacterial tests revealed inhibition zones of 5–12 mm at 10–50 µg/mL concentrations. These findings highlight the potential of *Pleurotus ostreatus*-derived nanoparticles as effective biopesticides with promising antibacterial applications.

Keywords: Nanoparticles, *Pleurotus ostreatus*, Mosquito control, Antibacterial activity, Thrombolytic effect

Introduction

Mosquitoes are key disease vectors, transmitting malaria, dengue, chikungunya, and other viruses, with females requiring blood meals to mature their eggs.¹ The key mosquito genera are *Anopheles*, *Culex*, and *Aedes*, with *Anopheles* being the only malaria carrier. Mosquitoes have a four-stage life cycle lasting 5 to 14 days. In temperate regions, eggs can enter diapause, delaying hatching for months until conditions improve.² The development of resistance in mosquitoes to synthetic insecticides and in *Plasmodium* parasites to antimalarial drugs significantly challenges malaria prevention and treatment, with widespread resistance to older medications undermining control efforts.³

Severe malaria can rapidly become fatal, highlighting the urgent need for effective treatments to eliminate *Plasmodium* parasites, prevent severe disease, and reduce the development of drug resistance.⁴

Pleurotus ostreatus, or oyster mushroom, is a widely cultivated edible mushroom known for its rich content of protein, carbohydrates, fibre, vitamins, and minerals, while being low in fat.⁵ Mushrooms, including *P. ostreatus*, are valued as nutraceuticals for their high-quality proteins, vitamins, and medicinal properties, such as antioxidant, anti-inflammatory, anticancer, and antimicrobial activities, making them significant in both culinary and medical research.^{6,7} The following properties listed makes *Pleurotus ostreatus* a strong candidate for insecticidal application. The biological synthesis of metallic nanoparticles, particularly noble metals like silver and gold, is gaining global interest for its applications in medicine and consumer products. Using herbal extracts and microorganisms for nanoparticle biosynthesis provides a simple, cost-effective, and eco-friendly alternative to traditional methods, enabling easy scalability and high yields.⁸ Some nanoparticles, such as Silver and gold, are widely studied for their optical and chemical properties, especially in biomedicine. Silver-gold alloy nanoparticles have diverse medical applications due to their low toxicity and improved biocompatibility through plant-based

*Corresponding author. Email: eaadebayo@lautech.edu.ng
Tel.: +2348038099092

Citation: Adebayo EA, Ayantola MM, Balogun HA, Lateef A, Azeez MA, Yekeen TA, Beukes LS, Matyumza N, Gueguim-Kana EB. *Anopheles gambiae* Control and Antibacterial Activity of Silver, Gold, and their Alloy Nanoparticles Synthesized Using *Pleurotus ostreatus*. Trop J Nat Prod Res. 2025; 9(11): 5795 – 5803 <https://doi.org/10.26538/tjnpr/v9i11.70>

Official Journal of Natural Product Research Group, Faculty of Pharmacy, University of Benin, Benin City, Nigeria

biosynthesis, including catalysis, antimicrobial activity, biofilm control, environmental toxin detection, and photothermal action.⁹

This study aims to synthesize silver nanoparticles (AgNPs), gold nanoparticles (AuNPs), and silver-gold alloy nanoparticles (Ag-AuNPs) using *Pleurotus ostreatus* and to evaluate their insecticidal (larvicidal, pupicidal, and adulticidal) and antibacterial potentials.

The objectives are to:

Synthesize and characterize AgNPs, AuNPs, and Ag-AuNPs using a green method. Evaluate their bioefficacy against different developmental stages of *Anopheles gambiae*, and assess their antibacterial activity against selected clinical pathogens.

Unlike previous studies with a focus on either larvicidal or antibacterial activities of biogenic nanoparticles, this study uniquely combines the green synthesis of nanoparticles from *Pleurotus ostreatus*, and assesses their multi-target bioactivity potential. The integration of nanoparticle-infused mosquito coils derived from agro-waste presents an innovative, eco-friendly vector control strategy with added environmental benefits.

Materials and Methods

The selected methods for the biosynthesis using *Pleurotus ostreatus*, and characterization via UV-Vis, FTIR, TEM, EDX, and SAED are well-established, eco-friendly techniques for nanoparticle synthesis and analysis. The mosquito bioassays (larvicidal, pupicidal, adulticidal) and antibacterial screening align directly with the study's goal of evaluating biomedical and entomological potentials of the synthesized nanoparticles.

Collection and Drying of Plant Materials

Fresh oyster mushrooms (*Pleurotus ostreatus*, accession number: MK751847) were obtained from the Microbiology and Biotechnology Laboratory at Ladoke Akintola University of Technology (8°8'0"N 4°16'0"E, 8°8'0"N 4°14'8"E). *P. ostreatus* (MK751847) was collected at LTC mushroom farm (7°46' N 4°34'E), Osogbo, Osun State, in 2020, cultivated, characterized to the species level, and registered in the GenBank database with accession number: MK751847.¹⁰ After cleaning, they were air-dried at (30 ± 2°C) to reduce moisture content and preserve bioactive compounds. Dried mushrooms were pulverized using an electric blender.

Extraction of *Pleurotus ostreatus*

To prepare the extract, 10 g of powdered *P. ostreatus* was mixed with 150 mL of sterile distilled water in a sealed cloth sack and left at room temperature (30 ± 2°C) for 24 hours. The mixture was then filtered using Whatman No. 1 filter paper and centrifuged at 4000 × g for 20 minutes. The resulting supernatant was stored in sterile universal bottles at 4°C for further use.¹¹

Biogenic synthesis of Nanoparticles (silver, gold, and silver-gold alloy)

Silver nanoparticles (AgNPs), gold nanoparticles (AuNPs), and silver-gold alloy nanoparticles (Ag-AuNPs) were synthesized by adding 1 mL of extract to 24 mL of 1 mM silver nitrate (AgNO₃) solutions, facilitating ion reduction.¹² The alloy was formed by mixing 1 mM AgNO₃ and 1 mM HAuCl₄ in a 4:1

ratio, followed by the addition of 1 mL of extract to 24 mL of the alloy solution. The reaction was allowed to proceed at room temperature (30 ± 2°C) for 2 hours, with color changes indicating nanoparticle formation.¹¹

Characterization of Nanoparticles

Pleurotus ostreatus-mediated nanoparticles (silver, gold, and silver-gold alloy) were characterized using various techniques. Colour changes indicated the biogenic reduction of silver and gold ions, quantitatively monitored by UV-Spectrophotometry (Model: Shimadzu UV-1800, Manufacturer: Shimadzu Corporation, Japan) to measure absorbance spectra. Fourier Transform Infrared (FTIR) spectroscopy (Model: Nicolet iS50; Manufacturer: Thermo Fisher Scientific, USA) identified functional groups in the samples by revealing characteristic peaks of green-synthesized silver nanoparticles, while Transmission Electron Microscopy (TEM) (Model: JEOL JEM-2100; Manufacturer: JEOL Ltd, Japan) confirmed nanoparticle size and morphology. Energy Dispersive X-ray (EDX) Spectroscopy (Model: Oxford X-MaxN 80; Manufacturer: Oxford Instruments United Kingdom (UK) and Selected Area Electron Diffraction (SAED) (Model: JEOL JEM-2100; Manufacturer: JEOL Ltd, Japan) provided elemental analysis and crystallinity information. Absorbance spectroscopy determines concentration using Beer-Lambert's Law. EDX provided elemental mapping, and TEM created magnified images by transmitting electrons through ultra-thin specimens.

Collection of *Anopheles gambiae* Larvae and Pupae

Larvae and pupae of *Anopheles gambiae* were collected from Ladoke Akintola University of Technology Ogbomosho, (8°8'0"N 4°16'0"E, 8°8'0"N 4°14'8"E). The species was authenticated at the Pure and Applied Biology Department and transported in clean plastic containers for larvicidal and pupicidal assays.

Vector Rearing

Bowl containers filled with water were placed in a controlled environment within the laboratory, with dry leaves and organic matter added to create suitable breeding conditions. After one month, *A. gambiae* larvae and pupae were observed. The larvae respired through posterior spiracles located on the eighth abdominal segment.¹³

Larvicidal and Pupicidal Activity

The larvicidal and pupicidal activity of AgNPs, AuNPs, and Ag-AuNPs was assessed at varying concentrations (1–20 µg/mL for larvae; 10–30 µg/mL for pupae). Groups of ten larvae or pupae were exposed to each concentration at room temperature (30 ± 2°C), and mortality was recorded at 12-hour and 24-hour intervals. Control experiments utilized sterile distilled water under identical conditions. Mortality percentages were calculated using the formula equation 1.¹⁴

$$\text{Percentage Mortality (\%)} = \frac{\text{Number of dead organisms}}{\text{Number of treated organisms}} \times 100\% \dots 1$$

Fume Effect on Adult *Anopheles* Mosquitoes

The fumigant effect was evaluated using AgNPs, as they exhibited the highest toxicity. A glass chamber (60 cm × 40 cm) with an iron mesh back was used for exposure. Mosquito coils were prepared using sawdust, coconut shell powder, starch, water, and AgNP extract. The mixture contained 10 mL of the extract, 0.8 g of sawdust, 0.3 g of coconut shell powder, and 0.7

g of starch, forming a semi-solid paste that was air-dried. The fumigant activity was tested at three AgNP concentrations (50 µg, 100 µg, and 170 µg), with negative control coils (without

Antibacterial Activity of AgNPs, AuNPs, and Ag-AuNPs

The antibacterial efficacy of the nanoparticles was tested against eight clinical bacterial isolates: *Escherichia coli* (ATCC 25922), *Escherichia coli* (stool), *Staphylococcus aureus* (Ear), *Pseudomonas aeruginosa* (ATCC 27853), *Proteus vulgaris* (Abdomen), *Listeria monocytogenes* (ATCC 19111), *Staphylococcus aureus* (ATCC 25923), and *Streptococcus pyogenes* (Sputum). Peptone water was used to cultivate the bacterial isolates and incubated for 24 h at 37°C. Cultures were then spread onto Mueller-Hinton agar plates, where wells were drilled for nanoparticle application at 10, 20, 30, 40, and 50 µg concentrations. The zones of inhibition were measured after incubating the plates at 37°C for 24 h. Positive controls included gentamicin (10 µg) for Gram-negative bacteria and erythromycin (5 µg) for Gram-positive bacteria. All discs were air-dried before bacterial inoculation.¹⁶

Statistical Analysis

The results of quantitative data analysis were expressed as mean ± SEM. One-way ANOVA was used to determine statistical significance using Duncan's Multiple Range Test, with p-values ≤ 0.05 considered statistically significant. Statistical software used was SPSS version 2010.

Results and Discussion

Biosynthesis of Nanoparticles (silver, gold, and silver-gold alloy)
Pleurotus ostreatus (PO) extracts mediated AgNPs, AuNPs, and Ag-AuNPs at 30 ± 2°C, resulting in light brown, purple, and dark brown hues after 10, 15, and 30 minutes. The colours intensified and stabilised after 40, 60, and 120 minutes. These findings are consistent with previous reports of purple¹⁷ and dark brown hues¹⁸ for AuNPs and Ag-AuNPs. Colloidal AgNPs, AuNPs, and Ag-AuNPs solutions have been reported to be a variety of hues, including light yellow, yellowish-brown, dark brown, pinkish, ruby red, yellowish, and purple. The colour change in metallic nanoparticles was caused by surface plasmon resonance. In this green synthesis, *Pleurotus ostreatus* performed bio-reducing and capping molecules that reduced silver ions to zero-valent silver and stabilised the nanoparticles to prevent aggregation.

Characterization of Biosynthesized Nanoparticles (AgNPs, AuNPs, and Ag-AuNPs)

UV-vis Spectroscopy

UV-vis spectroscopy of PO biosynthesised nanoparticles revealed a maximum absorbance at 430 nm for PO-AgNPs, 550 nm for PO-AuNPs, and 540 nm for PO-Ag/AuNPs (Figure 1). These numbers are most likely attributable to protein molecules in the extract. Previous research has reported that biosynthesized AgNPs, AuNPs, and Ag-AuNPs had wavelengths ranging from 330 to 800 nm.^{19,20,21}

Fourier Transform Infrared Spectroscopy (FTIR)

The FTIR absorption spectra of PO-AgNPs (Figure 2) showed strong peaks at 3788, 3262, 3037, 2549, 1736, 1592, 1441, 1109, and 711 cm⁻¹. The peak at 3262 represents O-H stretching of carboxylic acid, whereas the peak at 3037 represents C-H bonding of alkenes. The 1736 peak relates to C=O esters, the strong peak at 1441 is related to C-H bonding of methyl groups, and the peak at 1109 belongs to C-O stretching in carbohydrate rings.

nanoparticles) and commercially available mosquito coils serving as positive controls.¹⁵

The FTIR spectra of PO-AuNPs revealed peaks at 3780, 3292, 3051, 2547, 1728, 1442, 1078, and 678 cm⁻¹ (Figure 3). The peak at 3292 corresponds to carboxyl group O-H stretching, whereas the peak at 3051 represents alkene C-H stretching. The peak at 1728 corresponds to C=O stretching of amides or C=C stretching of alkenes, while the significant peak at 1442 is connected with C-H bonding of methyl groups. PO-Ag/AuNPs exhibited strong FTIR peaks at 3793, 3307, 3005, 2557, 1714, 1615, 1443, 1063, and 690 cm⁻¹ (Figure 4). The peak at 3307 indicates N-H bonding, while the 3005 peak corresponds to C-H of alkenes. The 1714 peak corresponds to C=O stretching of amides, the 1615 peak to C=C stretching of alkenes, and the 1443 peak to C-H stretching of methyl groups.

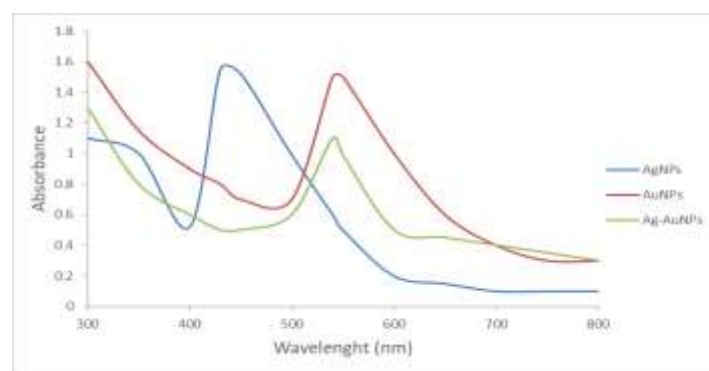


Figure 1: UV-vis spectroscopy of *Pleurotus ostreatus* Biosynthesized AgNPs, AuNPs, Ag-AuNPs

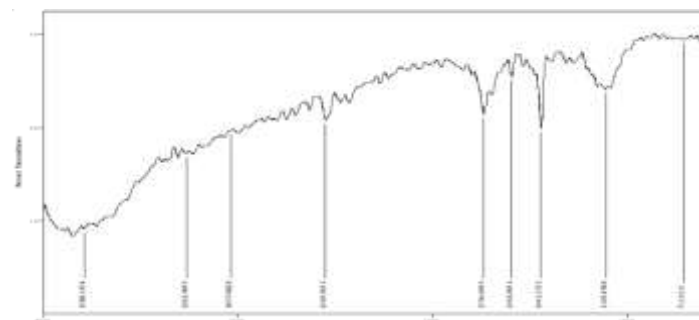


Figure 2: FTIR of Biosynthesized *Pleurotus ostreatus* AgNPs

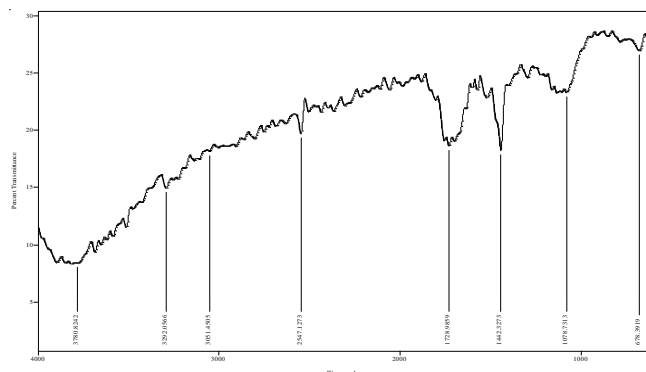


Figure 3: FTIR of Biosynthesized *Pleurotus ostreatus* AuNPs

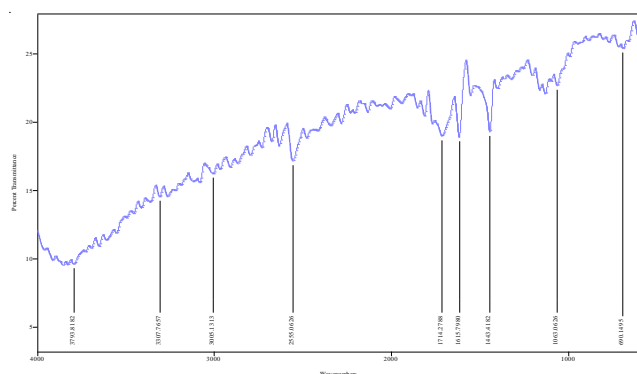


Figure 4: FTIR Biosynthesized *Pleurotus ostreatus* Ag-AuNPs

Transmission Electron Microscopy (TEM), Selected Area Electron Diffraction (SAED), and Energy Dispersive X-ray

The biosynthesized PO-AgNPs, PO-AuNPs, and PO-Ag-AuNPs TEM images are shown in Plates 1a, 2a, and 3a. PO-AgNPs, PO-AuNPs, and PO-Ag-AuNPs particles are polydispersed in distribution with various sizes from 25-37 nm, 10-50 nm, and 5- 20 nm, respectively. The shapes of the synthesized nanoparticles are mostly spherical with rod-like structures and occasionally form aggregates [17, 18, 19]. Plates 1b, 2b, and 3b showed a ring-shaped selected area electron diffraction pattern, which indicated that the nanoparticles are crystalline in form [18, 19]. EDX pattern showed the prevalence of Ag in the PO-AgNPs (Plate 1c) and gold in the PO-AuNPs solution (Plate 2c), while Plate 3c displays the prevalence of gold and silver in PAAg-AuNPs solution. It is obvious from these results that the bioreduction in gold and silver ions by the *Pleurotus ostreatus* extract led to the formation of PO-AgNPs, PO-AuNPs, and PO-Ag-AuNPs.

Larvicidal Activities

Pleurotus ostreatus (PO) silver, gold, and alloy nanoparticles (Figure 5) showed high larvicidal activity (70-100% against *Anopheles gambiae* larvae) at doses of 5-20 µg/ml. PO-AgNPs were very hazardous, causing 100% death within 12-24 hours at all tested doses. AuNPs exhibited little toxicity, with a maximum mortality rate of 40% at 20 µg/ml after 24 hours. However, at the same concentration and time, PO-Ag/AuNPs resulted in 100% death. Control samples subjected to distilled water exhibited no mortality.

The larvicidal actions demonstrated in this investigation are comparable to recent studies on plant extract-mediated AgNPs and Ag-AuNPs against *Anopheles* larvae.^{17,18,22} AgNPs displayed remarkable potency, producing 100% mortality at lower concentrations (15 and 20 µg/ml) within 12 hours, compared to 60 µg/ml over 72 hours as reported by Lateef *et al.* (2016). The high toxicity of AgNPs is likely due to their tiny size (18-80 nm), which allows them to easily pass through the insect's cuticle or digestive system, disrupting physiological processes and causing cell death.²³ Once inside cells, AgNPs can interact with macromolecules, causing cell death.²⁴ This shows that silver and gold nanoparticles produced by *Pleurotus ostreatus* have the potential as environmentally benign mosquito control agents. According to reports, metallic nanoparticles created by green synthesis play key roles in developing methods for combating medically and veterinarian-relevant mosquito species.²⁵

Pupicidal Activities

The pupicidal activities of the biosynthesized nanoparticles revealed that PO-AgNPs achieved 100% mortality in 12 and 24 hours at concentrations of 10-30 µg/ml (Figure 6). In contrast, PO-AuNPs had a maximum mortality of only 50% at 30 µg/ml in 24 hours (Figure 6). However, PO-Ag-AuNPs showed 100% mortality in 12 hours across all concentrations, and all the alloy nanoparticles demonstrated 100% pupicidal potency within 24 hours (Figure 6). No mortality was observed in the control groups exposed to distilled water or aqueous extracts. Statistical analysis confirmed that AgNPs' toxicity against pupae aligns with previous studies.^{26, 27} This toxicity is linked to abnormal morphology and swelling of the pupal integument, causing exoskeleton shrinkage during death.²⁸ The pupicidal potency of these biogenic nanoparticles suggests their potential use in malaria control by targeting larvae and pupae of *Plasmodium* vectors.

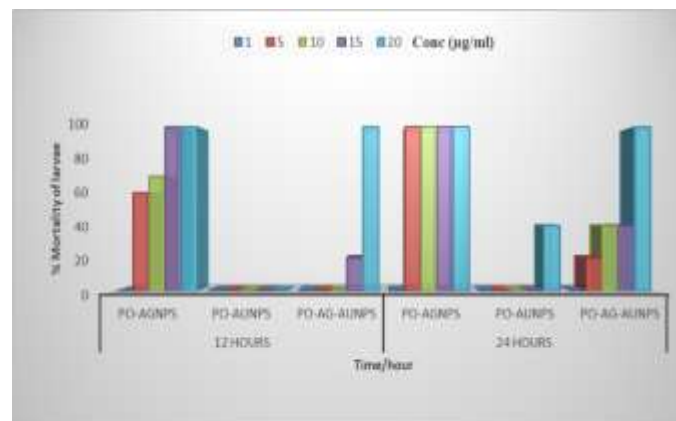


Figure 5: Percentage mortality (%) of larvae in 12 and 24 hours at different concentrations of synthesized AgNPs, AuNPs, and Ag-AuNPs using *Pleurotus ostreatus* (PO)

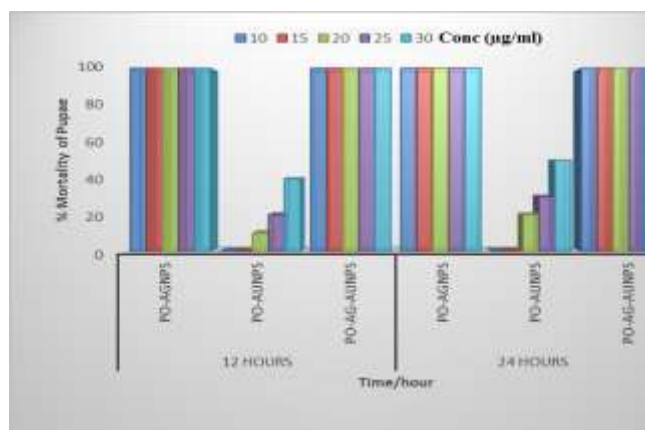


Figure 6: Percentage mortality (%) of Pupae in 12 and 24 hours at different concentrations of synthesized AgNPs, AuNPs, and Ag-AuNPs using *Pleurotus ostreatus* (PO)

Fume effect of Nano-Coil-based insecticide

The fume effect of coils doped with AgNPs (Plate 4) from *Pleurotus ostreatus* was reported in Table 1. PO-AgNPs showed no effect on adult mosquitoes at concentrations of 50 and 100 µg/ml over 6, 12, and 24 hours. However, at 170 µg/ml, 100% mortality was achieved within the time frames, with no mortality recorded in control coils without AgNPs. The maximum mortality of 100% was reached in 6 hours at 170 µg/ml, similar to the pyrethrin-based positive control. These results indicate that AgNPs have the potential as an eco-friendly mosquito control method, with the toxic vapours from burning nanoparticles affecting the mosquitoes' central nervous systems.²⁹ Using *Pleurotus ostreatus* as a bio-reduction in nanoparticle production and subsequent use as larvicidal, pupicidal, and adulticidal against *Anopheles mosquitoes* will increase the cultivation of *Pleurotus ostreatus*. Increased cultivation of *P. ostreatus* will reduce the waste in the environment, especially agro-waste, via bioconversion of waste to biomass (fruit body) to achieve a greener environment.

Nigeria is an agrarian country, generating several million tonnes of waste annually, constituting an environmental nuisance due to inappropriate disposal. The wastes, if utilized for mushroom biomass production, will assist in the conversion of waste to wealth. The added value is eco-friendly mosquito control using biologically synthesized nanoparticles, which could not pose any serious health effects in comparison with some chemically synthesized insecticides used for mosquito control.

Table 1: Percentage Mortality (%) of fume effect in 6 – 24 hours at different concentrations of synthesized AgNPs of PO.

Conc(µg/ml)	6 hours (%)	12 hours (%)	24 hours (%)
50	0	0	0
100	0	0	0
170	100	100	100
(-) Control	0	0	20
(+) Control	100	100	100

-negative + positive

Mosquito coils were formed using sawdust and coconut shell powder as major components for homogenization and burning. The usage of the two agro-waste will serve as a means of cleaning the environment. This study will contribute to Sustainable Development Goals (SDG) 3 (Good health and well-being), 9 (Innovation), and 13 (Climate action). The cultivation will guarantee the production of exotic food and insecticides for health promotion as well as eco-friendly means of managing agro-wastes through bioconversion to valuable products. The innovative aspect is bio-fabrication of nanoparticles from *Pleurotus ostreatus* as potent larvicidal, pupicidal, and adulticidal.

Antibacterial Activity

The nanoparticles of *Pleurotus ostreatus* (PO) showed antibacterial activity against eight clinical bacterial isolates (Tables 2-4), reducing their growth with zones of inhibition ranging from 5-12 mm at concentrations of 30-50 µg/ml. Antibacterial activity was found at concentrations of 30 µg/ml, 40 µg/ml, and 50 µg/ml, but was ineffective at doses below 30 µg/ml. PO-AgNPs had no significant antibacterial activity at 10 and 20 µg/ml but were effective at 30-50 µg/ml after 24 hours of incubation. At 50 µg/ml, the maximal inhibition zone was 10 mm against *Proteus vulgaris* (abdomen) and *Escherichia coli* (stool). The smallest zone of inhibition against *E. coli* (ATCC 25922) was 5 mm. Figure 6 shows that PO-AuNPs were ineffective at 10 and 20 µg/ml, with a maximum inhibition of 10 mm at 50 µg/ml against *E. coli* (stool). *Pleurotus ostreatus* alloy nanoparticles (Figure 6) had the largest inhibitory zone of 11 mm at the greatest dose (50 µg/ml), but were ineffective at concentrations below 30 µg/ml.

Table 2: Antibacterial inhibitory Activities of Biosynthesized AgNPs for PO at different concentrations

Clinical Organisms	Concentration (µg/ml)						+veC	-veC
	10	20	30	40	50			
<i>E. coli</i> (stool)	NA	NA	8.33 ± 0.33 ^{ab}	9.33 ± 0.33 ^b	10.33 ± 0.33 ^c		24	NA
<i>E. coli</i> (ATCC 25922)	NA	NA	5.33 ± 0.33 ^a	6 ± 0.577 ^{ab}	7.33 ± 0.33 ^{abc}		22	NA
<i>L. monocytogens</i> (ATCC 19111)	NA	NA	8 ± 0.577 ^{ab}	9 ± 0.577 ^b	9.33 ± 0.33 ^c		22	NA

<i>P. Vulgaris</i> (Abdomen)	NA	NA	8 ± 0.577^{ab}	9.33 ± 0.33^b	10.33 ± 0.33^c	26	NA
<i>P. aeruginosa</i> (ATCC 27853)	NA	NA	6 ± 0.577^a	8.33 ± 0.33^{ab}	8.33 ± 0.33^{abc}	25	NA
<i>S. aureus</i> (ATCC 25923)	NA	NA	7 ± 0.577^a	8.33 ± 0.33^{ab}	8 ± 0.577^{abc}	22	NA
<i>S. aureus</i> (Ear)	NA	NA	6.33 ± 0.33^a	7.33 ± 0.33^{ab}	9.67 ± 0.33^{bc}	20	NA
<i>S. pyogenes</i> (Sputum)	NA	NA	6.33 ± 0.33^a	7.33 ± 0.33^{ab}	7.33 ± 0.33^{abc}	25	NA

NA: (No Activity); Values are expressed as mean \pm SEM, mean denoted with different letters in the same column indicates a significant difference, $P < 0.05$; +veC (Positive control); -veC (Negative Control).

Table 3: Antibacterial inhibitory Activities of Biosynthesized AuNPs for PO at different concentrations

Clinical Organisms	Concentration ($\mu\text{g/ml}$)						
	10	20	30	40	50	+veC	-veC
<i>E. coli</i> (stool)	NA	NA	7.33 ± 0.33^a	9.33 ± 0.33^b	10 ± 0.577^c	24	NA
<i>E. coli</i> (ATCC 25922)	NA	NA	5.12 ± 0.24^a	6.51 ± 0.21^a	6.29 ± 0.25^a	22	NA
<i>L. monocytogens</i> (ATCC 19111)	NA	NA	5.43 ± 0.03^a	6.41 ± 0.65^a	7.45 ± 0.07^a	22	NA
<i>P. Vulgaris</i> (Abdomen)	NA	NA	6 ± 0.577^a	8.33 ± 0.33^b	9.33 ± 0.33^{ab}	26	NA
<i>P. aeruginosa</i> (ATCC 27853)	NA	NA	6 ± 0.577^a	7.33 ± 0.33^a	8 ± 0.577^b	25	NA
<i>S. aureus</i> (ATCC 25923)	NA	NA	6.62 ± 0.40^a	7.51 ± 0.44^a	8.43 ± 0.22^b	22	NA
<i>S. aureus</i> (Ear)	NA	NA	7.33 ± 0.33^a	8 ± 0.577^b	8 ± 0.577^b	20	NA
<i>S. pyogenes</i> (Sputum)	NA	NA	7.40 ± 0.24^a	8.56 ± 0.11^b	8.62 ± 0.45^b	25	NA

NA: (No Activity); Values are expressed as mean \pm SEM, mean denoted with different letters in the same column indicates a significant difference, $P < 0.05$; +ve C (Positive control); -ve C (Negative Control).

Table 4: Antibacterial inhibitory Activities of Biosynthesized Ag-AuNPs for PO at different concentrations

Clinical Organisms	Concentration ($\mu\text{g/ml}$)						
	10	20	30	40	50	+veC	-veC
<i>E. coli</i> (stool)	NA	NA	9.33 ± 0.33^{ab}	9.33 ± 0.33^{ab}	11 ± 0.577^c	24	NA
<i>E. coli</i> (ATCC 25922)	NA	NA	6.45 ± 0.11^a	7.62 ± 0.06^b	7.51 ± 0.44^b	22	NA
<i>L. monocytogens</i> (ATCC 19111)	NA	NA	6.0 ± 0.577^a	6.33 ± 0.33^a	7.21 ± 0.577^b	22	NA
<i>P. Vulgaris</i> (Abdomen)	NA	NA	5.67 ± 0.33^a	7 ± 0.577^b	9.33 ± 0.33^{ab}	26	NA
<i>P. aeruginosa</i> (ATCC 27853)	NA	NA	5.41 ± 0.27^a	7.71 ± 0.41^b	7.44 ± 0.70^b	25	NA
<i>S. aureus</i> (ATCC 25923)	NA	NA	6.24 ± 0.41^a	7.48 ± 0.17^b	8.81 ± 0.42^{ab}	22	NA
<i>S. aureus</i> (Ear)	NA	NA	5.61 ± 0.51^a	7.60 ± 0.41^b	8.55 ± 0.18^{ab}	20	NA
<i>S. pyogenes</i> (Sputum)	NA	NA	5.44 ± 0.50^a	6.43 ± 0.61^a	7.45 ± 0.42^b	25	NA

NA: (No Activity); Values are expressed as mean \pm SEM, mean denoted with different letters in the same column indicates a significant difference, $P < 0.05$; +ve C (Positive control); -ve C (Negative Control).

Biogenic nanoparticles demonstrated improved antibacterial efficacy against Gram-negative and Gram-positive bacteria at higher doses. Gram-negative bacteria are more sensitive to nanoparticles due to lipopolysaccharides interaction. Gram-positive and Gram-negative bacteria have been reported to show differing degrees of susceptibility to *Pleurotus* extracts.³⁰ The strong peptidoglycan layer in Gram-positive bacteria may inhibit penetration, although teichoic acid interactions may assist it.³¹ The nanoparticles demonstrated antibacterial activity, which is consistent with previous research on green-synthesized AgNPs, AuNPs, and Ag-AuNPs.^{32,33} Smaller, spherical nanoparticles have higher antibacterial activity.^{25,27} *Pleurotus ostreatus* biogenic nanoparticles showed prospects as alternatives to synthetic antibiotics in food and medicinal application.

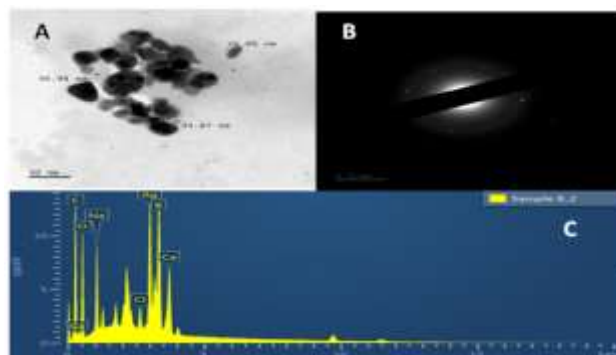


Plate 1: Transmission Electron Microscopy (TEM) of PO-AgNPs (A), Selected Area Electron Diffraction (SAED) of PO-AgNPs (B), Energy Dispersive X-ray of the Biosynthesized PO-AgNPs Nanoparticles (C) for *Pleurotus ostreatus* biosynthesized nanoparticles

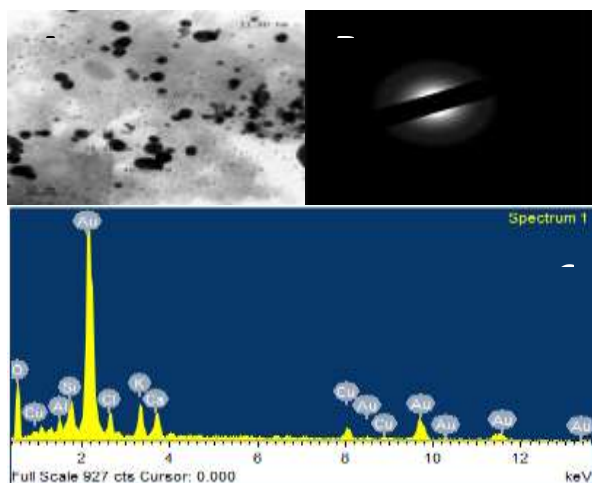


Plate 2: Transmission Electron Microscopy (TEM) of PO-AuNPs (A), Selected Area Electron Diffraction (SAED) of PO-AuNPs (B), Energy Dispersive X-ray of the Biosynthesized PO-AuNPs Nanoparticles (C) for *Pleurotus ostreatus* biosynthesized nanoparticles

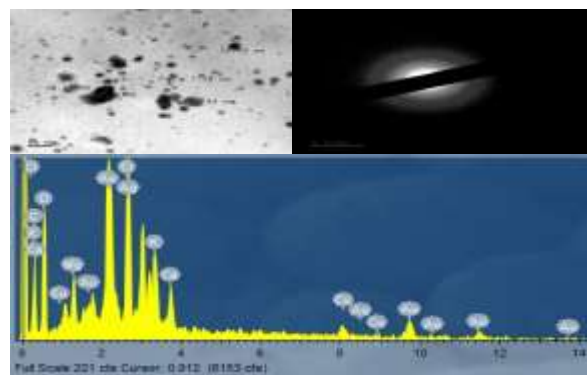


Plate 3: Transmission Electron Microscopy (TEM) of PO-AuNPs (A), Selected Area Electron Diffraction (SAED) of PO-AuNPs (B), Energy Dispersive X-ray of the Biosynthesized PO-AuNPs Nanoparticles (C) for *Pleurotus ostreatus* biosynthesized nanoparticles

Conclusion

This study demonstrates the green synthesis of AgNPs, AuNPs, and Ag-AuNPs using *Pleurotus ostreatus*, resulting in spherical, poly-dispersed nanoparticles (5-80 nm) with a crystalline structure. These nanoparticles exhibit significant larvicidal, pupicidal, and adulticidal effects against *Anopheles* mosquitoes, along with potent antibacterial. Further research is recommended to explore their potential in drug discovery.

Conflict of Interest

The authors declare no conflict of interest.

Authors' Declaration

The authors hereby declare that the work presented in this article are original and that any liability for claims relating to the content of this article will be borne by the authors.

Acknowledgments

The Management of Ladoke Akintola University of Technology, Ogbomoso, and TETFund, Nigeria, for 2023 National Research Fund (NRF) Intervention grant (TETF/ES/DR&D-CE/NRF2023/SETI/HSW/00871/VOL.1). Nigerian Stored Products Research Institute (NSPRI), Ilorin, Kwara State, Nigeria, and the Authority of KwaZulu-Natal University, South Africa, are appreciated for their collaboration, which enhanced the usage of equipment for Nanoparticle characterization and some biomedical assays. Graduate students who assisted in data collection during the study were equally appreciated. Also, Mrs. E.O. Adebayo and Mr. T.E. Akinwale, the English Language experts, are well appreciated for reading through the manuscript.

References

1. Nebbak A, Dabiré KR, Namountougou M, Sawadogo PS, Kientega M, Millogo AA, Baldet T. Study on the impact of insecticide resistance on mosquito vector control in sub-Saharan Africa. J. Vector Borne Dis. 2022; 59(2): 89–103.

2. Paton NI, Faiz MA, Karunajeewa HA, Von Seidlein L, Greenwood BM, White NJ. Challenges of antimalarial drug resistance and implications for treatment and control. *Lancet Infect. Dis.* 2022; 22(4): 345–359.
3. William T, Pinto J. The life cycle of mosquitoes and implications for control strategies. *Parasit. Vect.* 2012; 5: 45–52.
4. Nadjm B, Behrens RH. Severe malaria: Pathophysiology and treatment. *Clin. Infect. Dis.* 2012; 54(2): 169–174.
5. Piska K, Chmelova D, Dobranska G, Plachy V. Nutritional value and health benefits of *Pleurotus ostreatus*. *Food Chem.* 2016; 194: 1056–1062.
6. Patel Y, Naraian R, Singh VK. Medicinal properties of *Pleurotus* species (Oyster mushroom): A review. *World J. Fungal Res.* 2012; 8(3): 171–179.
7. Waktola Z, Temesgen D. Nutraceutical and medicinal values of mushrooms: A review. *Int. J. Med. Mushr.* 2020; 22(8): 781–795.
8. Siddiqi KS, Husen A. Green synthesis of noble metal nanoparticles using plant extracts. *Environ. Nanotechnol. Monit. Manag.* 2016; 5: 27–35.
9. Yallappa S, Manjanna J, Dhananjaya BL, Satyanarayan ND, Vishwanatha R, Singh BP, Adil S. Phytosynthesis of stable Au, Ag, and Au–Ag alloy nanoparticles using *Jatropha gossypifolia* leaf extract and their biological activities. *Mater. Sci. Eng. C.* 2015; 56: 264–271. [Doi: 10.1016/j.msec.2015.06.032](#)
10. Adebayo EA, Elkanah FA, Afolabi FJ, Ogundun OS, Alabi TF, Oduoye OT. Molecular characterization of most cultivated *Pleurotus* species in sub-western region Nigeria with development of cost effective cultivation protocol on palm oil waste. *Heliy.* 2021; 7: e06215. [Doi: 10.1016/j.heliyon.2021.e06215](#)
11. Rosyida VT, Hayati SN, Wiyono T, Darsih C, Ratih D. Effect of aqueous extraction method on total water-soluble polysaccharides content and phytochemical properties of white oyster mushroom (*Pleurotus ostreatus*). *IOP Conf. Ser.: Earth Environ. Sci.* 2024; 1377(1): 012064. [Doi: 10.1088/1755-1315/1377/1/012064](#)
12. Chaturvedi VK, Yadav N, Rai NK, Ellah NHA, Bohara RA, Rehan IF, Marraiki N, Batiha GE.-S, Hetta HF, Singh MP. *Pleurotus sajor-caju*-mediated synthesis of silver and gold nanoparticles active against colon cancer cell lines: A new era of herbonanocotics. *Mol.* 2020; 25(13): 3091. [Doi: 10.3390/molecules25133091](#)
13. Balogun HA, Ajala OO. Effect of phytochemical components of the leaf of *Moringa oleifera* on the development of *Anopheles gambiae*. *Trop. J. Phytochem. Pharm. Sci.* 2018; 3(6): 64–71. [Doi: 10.26538/tjpps/v3i6.2](#)
14. Abbott W S. A method of computing the effectiveness of an insecticide. *J. Econ. Entomol.* 1925; 18(2): 265–267. [Doi: 10.1093/jee/18.2.265a](#)
15. Zavala-Zapata V, Ramírez-Barrón SN, Sánchez-Borja M, Aguirre-Urbe LA, Delgado-Ortiz JC, Sánchez-Peña SR, Mayo-Hernández J, García-López JI, Vargas-Tovar JA, Hernández-Juárez A. Insecticide efficacy of green synthesis silver nanoparticles on *Diaphorina citri* Kuwayama (Hemiptera: Liviidae). *Insects.* 2024; 15(7): 469. [Doi: 10.3390/insects15070469](#)
16. Shakouie S, Milani S, Eskandarnejad M, Rahimi S, Froughreyhani M, Galedar R, Ranjbar M. Antimicrobial activity of tetraacetylenediamine-sodium perborate versus sodium hypochlorite against *Enterococcus faecalis*. *J. Dent. Res. Dent. Clin. Dent. Prosp.* 2016; 10: 43–47. [Doi: 10.15171/joddd.2015.007](#)
17. Kuppan P, Munusamy C, Manimegalai S. Synthesis and characterization of silver and gold nanoparticles using the mushroom *Pleurotus ostreatus*. *J. Nanosci. Nanotechnol.* 2015; 15(4): 2219–2226.
18. Lateef A, Ojo SA, Akinola PO. Green synthesis and pupicidal activities of alloy nanoparticles. *Parasitol. Int.* 2016; 65(4): 340–345.
19. Priyadarshini E, Pradhan N, Mandal A. Biosynthesis of silver nanoparticles using *Pleurotus ostreatus* extract. *Nanomed. J.* 2013; 9(1): 24–35.
20. Kumari M, Pandey S, Pandey A. Biosynthesis and characterization of silver nanoparticles using *Pleurotus ostreatus* extract. *Mater. Sci. Eng.* 2015; 51: 501–509.
21. Lateef A, Ojo SA, Akinola PO. Green synthesis and larvicidal activities of silver nanoparticles. *Biochem. Res. Int.* 2015; 206731. [Doi: 10.1155/2015/206731](#)
22. Musbau A, Lateef A, Ojo S. Larvicidal activities of biosynthesized nanoparticles against *Anopheles* larvae. *Biotechnol. Rep.* 2016. 12(3): 101–109.
23. Suresh A, Kumar P, Mukherjee A. Nanoparticles for mosquito vector control. *Environ. Nanotechnol. Monit. Manag.* 2018; 10: 256–270.
24. Badawy AM, Lotfy IM, El-Sherif HM. Green synthesis of silver nanoparticles and their application as antimicrobial agents. *J. Nanomater.* 2021; 439528. [Doi: 10.1155/2021/439528](#)
25. Benelli G, Mehlhorn H, Desneux N. Mosquito control with nanoparticle-based products: Present status and future perspectives. *Parasitol. Res.* 2017; 116: 325–335. [Doi: 10.1007/s00436-016-5296-0](#)
26. Hassan H, Mokhtar N, Ibrahim A. Pupicidal activity of biosynthesized nanoparticles against *Anopheles gambiae*. *J. Mosq. Res.* 2021; 5(1): 12–20.
27. Awad MA, Al-Qurashi AD, Alshawi SK, Said EA. Synthesis and characterization of silver nanoparticles for the control of mosquito-borne diseases. *J. Nanobiotechnol.* 2022; 20(1): 23. [Doi: 10.1186/s12951-022-01259-1](#)
28. Manimegalai S, Rajendran R, Kannan N. Silver nanoparticles in larvicidal applications: A review. *J. Parasit. Dis.* 2020; 44(1): 15–21.
29. Haldar P, Chakraborty D, Bhattacharjee S. Evaluation of fume effect on adult mosquitoes using silver nanoparticles. *J. Med. Entomol.* 2014; 51(4): 808–814.
30. Adebayo EA, Martinez-Carrera D, Morales P, Sobal M, Escudero H, Menesses ME, Avila-Nava A, Castillo I, Bonilla A. Comparative study of antioxidant and antimicrobial properties of edible mushrooms, *Pleurotus levis*, *P. ostreatus*, *P. pulmonarius*, and *P. tuber-regium*. *Int. J. Food Sci. Technol.* 2018; 53: 1316–1330. [Doi: 10.1111/ijfs.13723](#)

31. Jain D, Daima HK, Kachhwaha S, Kothari SL. Synthesis of plant-mediated silver nanoparticles and their applications: A review. *J. Nanomed. Nanotechnol.* 2015; 6(2): 285–298.
32. Adebayo EA, Abel MO, Oke A, Lateef A, Abayomi A, Oyatokun OD, Abisoye IP, Adiji DO, Fagbenro TV, Amusan BJA, Asafa TB, Beukes LS, Gueguim-Kana EB, Abbas SH. Biosynthesis of silver, gold, and silver-gold alloy nanoparticles using *Persea americana* fruit peel aqueous extract for their biomedical properties. *Nanotechnol. Environ. Eng.* 2019a; [Doi: 10.1007/s41204-019-0060-8](https://doi.org/10.1007/s41204-019-0060-8)
Adebayo EA, Ibikunle JB, Abel MO, Lateef A, Musbau AA, Adeboye OO, Ajala VA, Olowoporoku TB, Okunlola OC, Ogundele OA, Badmus AB, Asafa TB, Beukes LS, Gueguim-Kana EB, Abbas SH. Antimicrobial and antioxidant activity of silver, gold, and silver-gold alloy nanoparticles photosynthesized using the extract of *Opuntia ficus-indica*. *Res. Adv. Mater. Sci.* 2019b; [Doi: 10.1515/rams-2019-0039](https://doi.org/10.1515/rams-2019-0039)
33. Halder P, Chakraborty D, Bhattacharjee S. Evaluation of fume effect on adult mosquitoes using silver nanoparticles. *J. Med. Entomol.* 2014; 51(4): 808–814.
34. Adebayo EA, Martinez-Carrera D, Morales P, Sobal M, Escudero H, Meneses ME, Avila-Nava A, Castillo I, Bonilla A. Comparative study of antioxidant and antimicrobial properties of edible mushrooms, *Pleurotus levis*, *P. ostreatus*, *P. pulmonarius*, and *P. tuber-regium*. *Int. J. Food Sci. Technol.* 2018; 53; 1316–1330. [Doi: 10.1111/ijfs.13723](https://doi.org/10.1111/ijfs.13723)
35. Jain D, Daima HK, Kachhwaha S, Kothari SL. Synthesis of plant-mediated silver nanoparticles and their applications: A review. *J. Nanomed. Nanotechnol.* 2015; 6(2): 285–298.
36. Adebayo EA, Abel MO, Oke A, Lateef A, Abayomi A, Oyatokun OD, Abisoye IP, Adiji DO, Fagbenro TV, Amusan BJA, Asafa TB, Beukes LS, Gueguim-Kana EB, Abbas SH. Biosynthesis of silver, gold, and silver-gold alloy nanoparticles using *Persea americana* fruit peel aqueous extract for their biomedical properties. *Nanotechnol. Environ. Eng.* 2019a; [Doi: 10.1007/s41204-019-0060-8](https://doi.org/10.1007/s41204-019-0060-8)
37. Adebayo EA, Ibikunle JB, Abel MO, Lateef A, Musbau AA, Adeboye OO, Ajala VA, Olowoporoku TB, Okunlola OC, Ogundele OA, Badmus AB, Asafa TB, Beukes LS, Gueguim-Kana EB, Abbas SH. Antimicrobial and antioxidant activity of silver, gold, and silver-gold alloy nanoparticles photosynthesized using the extract of *Opuntia ficus-indica*. *Res. Adv. Mater. Sci.* 2019b; [Doi: 10.1515/rams-2019-0039](https://doi.org/10.1515/rams-2019-0039)